Rate Constants for the Reactions of Hydroxyl and Hydroperoxyl Radicals with Ozone

Abstract. *Chain decomposition of ozone by hydroxyl and hydroperoxyl radicals has been observed. The rate constant at 300°K for* $OH + O_3 \rightarrow HO_2 + O_2$ *is* 8×10^{-14} *cubic centimeters per second. The rate constant for* $HO_2 + O_3 \rightarrow OH + 2O_2$ *is* 3×10^{-15} *cubic centimeters per second. These results have implications concerning stratospheric ozone.*

Atmospheric modelers have concluded that water effects are unimportant in the destruction of atmospheric ozone (*1*). The results reported here suggest that such a conclusion may be premature.

The "wet chemistry" model of atmospheric ozone is based largely on the reactions

$$OH + O_3 \rightarrow HO_2 + O_2 \quad (1)$$

$$HO_2 + O_3 \rightarrow OH + 2O_2 \quad (2)$$

which were suggested by Norrish and co-workers (*2*) to explain the effect of water on laboratory ozone photolysis. That mechanism has been questioned (*3*), however, particularly since the report of Langley and McGrath (*4*) that the rate constant for reaction 1 is less than 10^{-16} cm^3 sec^{-1}. This value is, however, considerably lower than would have been expected on the basis of the experiments of Coltharp *et al.* (*5*). These workers found that OH in excited vibrational levels $v = 2$ to $v = 9$ reacts rapidly with O_3 (the rate constant, k, ranging from 2×10^{-12} cm^3 sec^{-1} for $v = 2$ to 8×10^{-12} cm^3 sec^{-1} for $v = 9$). They were unable to measure k for $v = 0$, but extrapolation of their data from higher levels suggested a value generally in agreement with the upper limit of 5×10^{-13} cm^3 sec^{-1} established by Kaufman (*6*).

This report gives a new measurement of k for reaction 1, k_1, which is about 10^3 higher than the Langley and McGrath value. A value of k_2 is also derived.

The experiment involved photolysis of O_2-H_2O mixtures at 1849 Å. The quartz photolysis cell had a diameter of 15 cm and a length of 90 cm, and was irradiated end-on. The photolysis mixture was 300 torr of O_2 and 4.6 torr of H_2O, under which conditions the water absorbed light at a rate 1/9 that of O_2. This calculation is based on an extinction coefficient (1849 Å) of 2.1 cm^{-1} atm^{-1} for water and 0.29 cm^{-1} atm^{-1} for O_2, as determined in the course of this work. The light source was a low-pressure mercury lamp combined with an O_2-O_3 filter (*7*), which screened out essentially all of the 2537-Å light. This lamp-filter combination produces a constant intensity of 1849-Å light for indefinite periods of time. The principal advantage, for the present purposes, is that O_3 photolysis at 2537 Å is avoided, so that ozone does not become a significant source of atomic oxygen. At low O_3 concentrations, absorption of 1849-Å light is negligible compared to absorption by O_2 and H_2O, so that O_3 is photochemically inert in the mixture. The O_2 was Matheson "ultra high purity" grade, containing less than 2 parts of H_2O per million.

Ozone is produced by photodissociation of O_2, and all oxygen atoms are scavenged by O_2 (at the low O_3/O_2 ratios of this experiment), so that O_3 production is quite linear with time, in the absence of H_2O (see Fig. 1). With H_2O present, the O_3 production rate declines as the O_3 concentration increases, until a steady state is reached, which then persists indefinitely. The O_3 concentrations show no appreciable decline with the lamp off. Since H_2O photolysis produces odd hydrogen radicals only 1/9 as fast as O_3 is produced by the O_2 photolysis, it follows immediately that chain decomposition of O_3 is occurring. Further, the chain must be carried by OH and HO_2 radicals (reactions 1 and 2) because almost all (approximately 98 percent) of the H atoms are scavenged by O_2 at the O_2/O_3 ratios obtained. This result appears to be a well-defined case of O_3 chain decomposition by the Norrish mechanism.

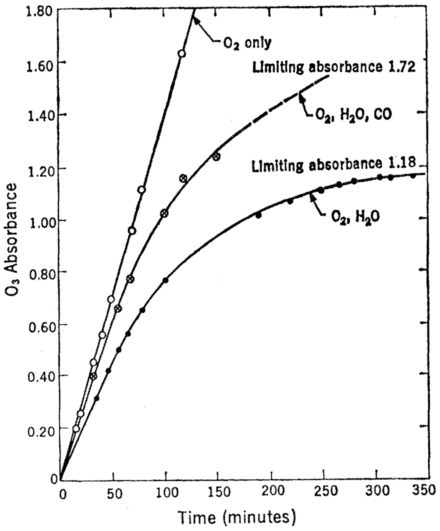

Fig. 1. Time dependence of O_3 concentrations for irradiation of various mixtures at 1849 Å. For pure O_2, the production of O_3 is linear with time. With added water, a steady state is reached when the rate of O_3 destruction by OH and HO_2 radicals equals the rate of production. Addition of excess CO (CO $\gg$ O_3) converts OH to HO_2, and a different steady state results. In this apparatus, 1 absorbance unit corresponds to 67 μm of O_3.

A mechanism which accounts for these observations is as follows, where the wavelength, λ, is 1849 Å; $I_a^{O_2}$ is the intensity of light absorbed by O_2; $I_a^{H_2O}$ is the intensity of light absorbed by H_2O; and M is a third body.

$$O_2 + \lambda \xrightarrow{I_a^{O_2}} O + O \text{ (ground state)} \quad (3)$$

$$H_2O + \lambda \xrightarrow{I_a^{H_2O}} H + OH \quad (4)$$

$$O + O_2 + M \xrightarrow{k_5} O_3 + M \quad (5)$$

$$H + O_2 + M \xrightarrow{k_6} HO_2 + M \quad (6)$$

$$H + O_3 \xrightarrow{k_7} OH + O_2 \text{ (negligible)} \quad (7)$$

$$OH + O_3 \xrightarrow{k_1} HO_2 + O_2 \quad (1)$$

$$HO_2 + O_3 \xrightarrow{k_2} OH + 2O_2 \quad (2)$$

$$OH + HO_2 \xrightarrow{k_8} H_2O + O_2 \quad (8)$$

$$HO_2 + HO_2 \xrightarrow{k_9} H_2O_2 + O_2 \quad (9)$$

$$OH + H_2O_2 \xrightarrow{k_{10}} H_2O + HO_2 \quad (10)$$

Photolysis of H_2O_2 has been neglected, for reasons described later.

Under steady-state conditions we have k_1 [OH] $= k_2$ [HO_2], where the brackets denote concentration, and the O_3 concentration is given by (neglecting reaction 7)

$$[O_3]_{ss} = \frac{2I_a^{O_2}}{k_1[OH] + k_2[HO_2]} = \frac{I_a^{O_2}}{k_2[HO_2]} \quad (11)$$

The individual rate constants for reactions 1 and 2 were measured by experiments involving the addition of CO to the mixture, which has the effect of converting OH to HO_2:

$$OH + CO \rightarrow H + CO_2 \quad (12)$$

$$H + O_2 + M \rightarrow HO_2 + M \quad (6)$$

With the addition of sufficient CO to scavenge all the OH ($CO \gg O_3$), a different O_3 steady state is obtained, as shown in Fig. 1. The limiting O_3 absorbance is 1.72 (115 μm), as compared to 1.18 (79 μm) in the absence of CO. The O_3 steady state with excess CO is determined by the rates of reaction 2 and the chain termination step, reaction 9.

In the limit of excess CO, the O_3 steady state is given by (again neglecting reaction 7)

$$[O_3]_{ss} = \frac{2I_a^{O_2}}{k_2[HO_2]_{ss}} \qquad (13)$$

If reaction 9 is the only termination path, then $[HO_2]_{ss}$ can be calculated, since

$$k_9[HO_2]^2_{ss} = I_a^{H_2O} \qquad (14)$$

and $k_9 \sim 10^{-11}$ cm^3 sec^{-1} (*8*).

Inserting the known quantities in Eqs. 13 and 14 yields $k_2 \sim 2 \times 10^{-15}$ cm^3 sec^{-1}. However, because of nonuniform light absorption, this value is expected to be an underestimation of the true k_2. For experiments with successively lower total absorption of light, k_2 approached the limiting value

$$k_2 = 3 \times 10^{-15} \text{ cm}^3 \text{ sec}^{-1} \qquad (15)$$

The rate constant k_1 can be determined in two ways. The first method is based on competition between CO and O_3 for OH. The rate of reaction 12 is known (*9*): $k_{12} = 5.1 \times 10^{-13} \exp(-300/T)$ cm^3 sec^{-1}, where T is absolute temperature. Figure 2 shows the effect of adding different concentrations of CO to an O_2-H_2O mixture which has reached steady state. Suppression of the OH concentration by CO causes an imbalance in the rates of ozone production and destruction, and therefore the ozone concentration immediately begins to rise. Both the initial slope and the maximum O_3 concentration attained depend on the extent to which CO competes with O_3 for OH. The latter data are more difficult to interpret because the CO is consumed to an appreciable extent, so that the O_3 concentration eventually returns to the starting value in the CO-free case. The best fit of the initial slope data is obtained for $k_1 = 0.45k_{12}$, or

$$k_1 = 8 \times 10^{-14} \text{ cm}^3 \text{ sec}^{-1} \text{ (300°K)} \qquad (16)$$

A second calculation of k_1 utilizes the fact that the absolute radical concentrations depend on the ratio OH/HO_2, because there are two termination steps whose rate must equal the rate of water photolysis:

$$k_8[OH][HO_2] + k_9[HO_2]^2 = I_a^{H_2O} \qquad (17)$$

The chain does not result in any net production or destruction of radicals, but does determine their ratio, so that $OH/HO_2 = k_2/k_1$. When excess CO is added, OH is suppressed and reaction 8 becomes negligible as a termination step. The HO_2 concentration therefore rises, and the relative HO_2 concentrations in the presence and absence of CO can be inferred from the O_3 steady-state values under the respective conditions, by using Eqs. 11 and 13.

$$\frac{[HO_2]^{CO}_{ss}}{[HO_2]^{0}_{ss}} = 2\,\frac{[O_3]^{0}_{ss}}{[O_3]^{CO}_{ss}} \qquad (18)$$

The superscripts 0 and CO refer to no CO and excess CO, respectively.

When these relationships are combined, it follows that

$$\frac{k_8k_2}{k_9k_1} = 4\left(\frac{[O_8]^{0}_{ss}}{[O_3]^{CO}_{ss}}\right)^2 - 1 \qquad (19)$$

Thus, with the experimental result that $[O_3]^{CO}_{ss} = 1.46\,[O_3]^{0}_{ss}$, it is found that

$$k_1 = 1.13\; k_2\,\frac{k_8}{k_9} \qquad (20)$$

From (*8*), $k_8/k_9 = 21$. Therefore, with the previous result that $k_2 = 3 \times 10^{-15}$ cm^3 sec^{-1},

$$k_1 = 7 \times 10^{-14} \text{ cm}^3 \text{ sec}^{-1} \text{ (300°K)} \qquad (21)$$

The average value from method one and method two, which are probably equally reliable, is thus 7.5×10^{-14} cm^3 sec^{-1}. Anderson and Kaufman (*10*) have obtained the value $k_1 = (5.5 \pm 1.5) \times 10^{-14}$ cm^3 sec^{-1} by using a quite different experimental method.

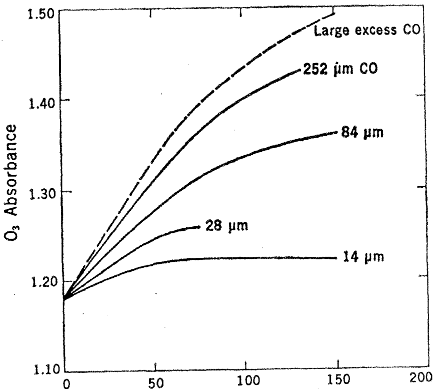

Fig. 2. Addition of varying CO concentrations to O_2-H_2O mixtures at steady state. These data show that CO competes effectively with O_3 for OH only when the CO concentration is comparable to the O_3 concentration.

The reliability of the present values for k_1 and k_2 depends primarily on the correctness of the proposed mechanism. There appears to be little doubt regarding the role of reaction 1, particularly in view of the close agreement between the present results for k_1 and the Anderson and Kaufman value. The identification of HO_2 as a chain carrier is based on the fact that no other path is available to account for the observed rate of O_3 destruction (or, as would be equivalent, of atomic oxygen destruction). No species, including O_3, H_2O_2, HO_2, or CO, is present in sufficient concentration, or can be produced at a sufficient rate, to react appreciably with atomic oxygen, other than O_2. Also, the consistency of k_1 as calculated from method two, in which the roles of OH and HO_2 are assumed, with k_1 determined in other ways supports the proposed mechanism.

Experiments were carried out to test the assumption that radical-radical reactions (reactions 8 and 9) are the only termination steps. If this is the case, the mechanism predicts that the ozone steady state should be proportional to the square root of the light intensity, in both the presence and absence of CO. The experimental results were that, for a factor of 2 decrease in light intensity, the respective changes in $[O_3]_{ss}$ were 1.39 and 1.37, in good agreement with the predicted $2^{1/2}$ dependence. The mechanism also predicts (to a close approximation) that $[O_3]_{ss}$ should be inversely proportional to $[H_2O]^{1/2}$. Variation of the partial pressure of water in the range 1.5 to 12.6 torr (five separate experiments) verified this prediction remarkably well. These findings appear to rule out any first-order termination steps. If there is any second-order radical termination on the walls, then the reported k_2 would be lower than the true value.

Hydrogen peroxide is formed by reaction 9 and reaches a steady state given by

$$[H_2O_2]_{ss} = \frac{k_9[HO_2]^2}{k_{10}[OH]} \leqq \frac{I_a^{H_2O}}{k_{10}[OH]} \qquad (22)$$

To a close approximation, and with $k_{10} = 10^{-12}$ cm^3 sec^{-1} (*11*),

$$\frac{[H_2O_2]_{ss}}{[O_3]_{ss}} = \frac{I_a^{H_2O}k_1}{I_a^{O_2}k_{10}} \sim \frac{1}{130} \qquad (23)$$

This low value of $[H_2O_2]_{ss}$ explains why photolysis of that product, which would serve as an additional source of OH, is unimportant in these experiments. At lower OH concentrations, as in the experiments with added CO, H_2O_2 will reach higher concentrations. However, no effects attributable to H_2O_2 have been observed in the experiments.

WILLIAM B. DEMORE
Jet Propulsion Laboratory,
Pasadena, California 91103

References and Notes

1. See, for example, A. E. Barrington, Ed., *Proceedings of the Survey Conference* (Climatic Impact Assessment Program, Department of Transportation, Washington, D.C., 1972).
2. R. G. W. Norrish and R. P. Wayne, *Proc. Roy. Soc. London Ser. A* **288**, 361 (1965); W. D. McGrath and R. G. W. Norrish, *ibid.* **254**, 317 (1960); *Nature* **182**, 235 (1958).
3. W. B. DeMore, *J. Chem. Phys.* **46**, 813 (1967).
4. K. R. Langley and W. D. McGrath, *Planet. Space Sci.* **19**, 413 (1971).
5. R. N. Coltharp, S. D. Worley, A. E. Potter, *Appl. Opt.* **10**, 1786 (1971).
6. F. Kaufman, *Ann. Geophys.* **20**, 106 (1964).
7. The filter consists of a 2-cm path of O_2 at 1 atm, cooled to about −5°C. The steady-state absorbance of O_3 is more than 4.0.
8. C. J. Hochanadel, J. A. Ghormley, P. J. Ogren, *J. Chem. Phys.* **56**, 4426 (1972).
9. W. E. Wilson, Jr., *J. Phys. Chem. Ref. Data* **1**, 535 (1972).
10. J. Anderson and F. Kaufman, *Chem. Phys. Lett.*, in press.
11. N. R. Greiner, *J. Phys. Chem.* **72**, 406 (1968).
12. This report presents the results of one phase of research carried out at the Jet Propulsion Laboratory, California Institute of Technology, under NASA contract NAS7-100. I am grateful to N. Davidson and H. Ford for helpful conversations and to F. Kaufman for the disclosure of recent results concerning reaction 1.

4 December 1972; revised 20 February 1973 ■

Magnetospheric Dayside Cusp: A Topside View of Its 6300-Angstrom Atomic Oxygen Emission

Abstract. *An interference filter photometer on the ISIS-II spacecraft generates global maps of the atomic oxygen emission at 6300 angstroms from the ionosphere. The most prominent feature observed is a band of permanent red aurora on the dayside of the earth, centered on magnetic noon at about 78 degrees magnetic (invariant) latitude, brighter than the quiet-time nightside aurora.*

Our knowledge of the detailed characteristics of the earth's magnetosphere has rapidly increased in recent years. One important aspect now receiving attention is the dayside cusp. This name has been given to the magnetic neutral point on the dayside, a demarcation dividing the magnetic field lines which turn equatorward and close on the dayside from those which stream over the pole into the tail of the magnetosphere. It appears that solar plasma can enter the magnetosphere unimpeded at this point, flowing down to ionospheric levels. Using all-sky camera data from a number of stations, Feldstein (*1*) constructed an "instantaneous" auroral distribution pattern now called the auroral oval, and showed that it closed on the dayside at about 79° magnetic invariant latitude. Soon afterward, satellites carrying detectors of low-energy electrons detected a region of "soft" precipitation on the dayside (*2*). Later particle observations (*3*) identified this precipitation with the dayside neutral point or cusp, and Hoffman and Berko (*4*) related their particle observations to the ground-based observation of discrete auroral forms. Since dayside auroras can be observed at local noon, albeit in rather inaccessible geographical regions, a series of aircraft observations were carried out (*5–8*). Heikkila *et al.* (*9*) have provided a detailed documentation of the relevant particle and optical characteristics. The precipitation consists of isotropic 100-ev electrons and 300-ev to 3-kev protons. The protons are considered to identify the cusp most sharply, which occurs between about 79° and 81° invariant latitude, depending on the level of activity. It is recognized that the cusp extends well to both sides of local noon, but the existing knowledge of its longitudinal extent has been built up from a number of satellite passes made at different times.

This is a report of an optical observation of the entire dayside cusp region, taken in "snapshot" fashion during a single pass with the second international satellite for ionospheric studies, ISIS-II. The spacecraft was launched on 1 April 1971 into a near-circular near-polar orbit at a nominal altitude of 1400 km. The instrumentation is similar to that of ISIS-I (*10*), but one of the new instruments aboard is the red line photometer (*11*), designed to measure the global distribution of the 6300-Å emission of atomic oxygen, OI. The photometer looks perpendicular to the spacecraft spin axis with two optical axes, 180° apart, characterized by spectral bandwidths of about 10 and 88 Å. The two optical channels can share the same photomultiplier and electronics, since when one channel views the earth the other scans the dark sky. The spin-stabilized spacecraft has a rotation period of about 18 seconds, during which the spacecraft moves approximately 120 km. The photometer has a field of view of 2.5° angular diameter or 60 km when looking vertically downward on the earth. With the spin axis in the orbit plane, the combined rotation and orbital motion generates a raster-like scan across the earth, generating maps in both wavelength channels. These can be combined to extract the white light background and so to generate a global map in the 6300-Å emission.

On 14 December 1971, the spacecraft spin axis had been maneuvered by magnetic torquing to within 30° of the orbit plane and a declination of −10°; the orbit plane was then close to the noon-midnight meridian. This provided very favorable viewing conditions for the auroral oval in the dark northern polar cap. The purpose of this report is to present the polar map obtained from 05:18 to 05:40 U.T. in a single pass by using the ground stations at Resolute Bay, Northwest Territories, and Ottawa, Canada; practically the entire auroral oval is visible, and particularly the 6300-Å emission from the dayside cusp. The value of the observation is that it makes available an essentially instantaneous picture of a region that has dynamic characteristics.

The data are presented in Fig. 1 in the form of a spin map (*12*), generated by the computer line printer. In this map, one line of print corresponds to one rotation of the spacecraft; the two scans of different bandwidths obtained from subsequent half-rotations have been combined to present the extracted 6300-Å emission as single scans in which the intensity is represented by the density of the symbol used. The leading limb of the emission is forced to coincide with the left edge of the page and the trailing limb falls where it occurs, somewhere inside the right edge. That limb is evident in Fig. 1 owing to the enhancement of tangential viewing; a simple cosine correction is applied to the data, but this correction is inadequate right at the limb, for several reasons. The dayside cusp ap-